

This item was submitted to Loughborough's Institutional Repository (<https://dspace.lboro.ac.uk/>) by the author and is made available under the following Creative Commons Licence conditions.



CC creative commons
COMMONS DEED

Attribution-NonCommercial-NoDerivs 2.5

You are free:

- to copy, distribute, display, and perform the work

Under the following conditions:

BY: **Attribution.** You must attribute the work in the manner specified by the author or licensor.

Noncommercial. You may not use this work for commercial purposes.

No Derivative Works. You may not alter, transform, or build upon this work.

- For any reuse or distribution, you must make clear to others the license terms of this work.
- Any of these conditions can be waived if you get permission from the copyright holder.

Your fair use and other rights are in no way affected by the above.

This is a human-readable summary of the [Legal Code \(the full license\)](#).

[Disclaimer](#) 

For the full text of this licence, please go to:
<http://creativecommons.org/licenses/by-nc-nd/2.5/>

Mitigating plasma constriction using dielectric barriers in radio-frequency atmospheric pressure glow discharges

J. J. Shi, D. W. Liu, and M. G. Kong^{a)}

Department of Electronic and Electrical Engineering, Loughborough University, Loughborough, Leicestershire LE11 3TU, United Kingdom

(Received 11 October 2006; accepted 13 December 2006; published online 19 January 2007)

It is known that radio-frequency (rf) atmospheric glow discharges with bare electrodes are susceptible to plasma constriction at large discharge currents. This is undesirable for large-scale applications, even though large currents usually lead to abundant plasma reactive species and high application efficiency. In this letter, an experimental investigation is presented to demonstrate that plasma constriction can be mitigated by introducing dielectric barriers to the electrodes. The resulting atmospheric rf dielectric-barrier discharge is shown to operate in the γ mode of large discharge current while maintaining its discharge volume. This improves significantly plasma stability and the application potential. © 2007 American Institute of Physics.

[DOI: 10.1063/1.2432233]

Large-volume atmospheric pressure glow discharges (APGD's) generated at radio frequencies (rf's) have recently attracted much attention, primarily because they offer a low-voltage and chamberless route to numerous industrial and biomedical applications.^{1–8} Employing a pair of bare electrodes, rf APGD's are often sustained in either the α mode of small currents or the γ mode of large currents.^{3,5,8,9} These two glow modes exhibit significant difference in their discharge characteristics, particularly plasma stability and plasma reactivity. Critical for reliable applications, plasma stability describes the ability of a gas discharge to maintain its uniformity in a large volume. Plasma reactivity, on the other hand, measures its ability to produce large quantities of reactive plasma species for high application efficiency. Significantly, a key challenge for the APGD technology is that their plasma stability and plasma reactivity are often mutually exclusive of each other.¹⁰ In the case of rf APGD, the stability of the α mode is robust but achieved only by restricting the discharge current.^{5,9} Inevitably, the low-current nature of the α mode leads to low concentrations of reactive species and poor plasma reactivity.¹⁰ One common method to improve plasma reactivity is to increase the discharge current, thus moving rf APGD into the γ mode so that gas ionization is enhanced substantially.^{5,9} While this leads to abundant reactive plasma species, it can simultaneously shrink the rf glow discharge into a constricted plasma column in a manner similar to that in rf glow discharges at medium gas pressures.¹¹ In fact, it is difficult to attain large-volume rf APGD in the γ mode without plasma constriction. This compromises the benefits of APGD for large-volume applications and renders high plasma reactivity redundant.

Recently, we proposed theoretically the use of dielectric barriers in rf APGD to control their plasma stability even though the generation of conventional rf APGD does not require dielectric barriers.¹² This technique could potentially be used to control plasma constriction in rf APGD. In this letter, we present an experimental study to demonstrate that dielectric barriers can mitigate plasma constriction in rf at-

mospheric glow discharges, thus allowing for stable plasma operation at large discharge currents. For future reference, we refer conventional rf atmospheric glow discharges with bare electrodes to as rf APGD and those with dielectrically insulated electrodes to as atmospheric rf dielectric-barrier discharges.

The rf DBD considered here was generated between two parallel stainless-steel plates each covered with a ceramic sheet of 0.5 mm in thickness and 9.0 in relative permittivity. The electrode diameter was 20 mm, and the gas gap was fixed at 2.4 mm. The electrode unit was enclosed in a Perspex box with a helium flow of 5 SLM (standard liters per minute) at 760 torr. To produce a comparable rf APGD, the same electrode unit was employed without the ceramic sheets and with the gas gap fixed at 2.4 mm. For both cases, one electrode was powered, via a homemade impedance matching network, by a radio-frequency power source system, in which a 5 MHz sinusoidal signal was generated by a function generator (Tektronix AFG 3102) and then amplified by a power amplifier (AR 150A100B). The discharge current and the applied voltage were measured by a wideband current probe (Tektronix P6021) and a wideband voltage probe (Tektronix P6015A), and their wave forms were recorded on a digital oscilloscope (Tektronix TDS 3034B). With the triggering signal, an intensified charge-coupled device (iCCD) camera (Andor i-Star DH720) was used to capture the plasma images with an exposure time of 10 ns. Optical emission spectrum was obtained using a spectrometer system (Andor Shamrock) with a focal length of 0.3 m and a grating of 600 grooves/mm.

Typical traces of the applied voltage and the discharge current of the rf DBD are shown in Fig. 1. Both the discharge current and the applied voltage are predominately sinusoidal, with the current leading the voltage by a phase shift of less than 90°. Their wave forms are consistent with the simulation results¹² and similar to those found in rf APGD with bare electrodes.^{3,8} In contrast, their sinusoidal character is distinctly different from the pulselike current wave form of conventional kilohertz atmospheric DBD.^{13,14} Also shown in Fig. 1 is the iCCD trigger pulse of 5 V and subnanosecond pulse-rising phase. To illustrate the benefits of the dielectric

^{a)} Author to whom correspondence should be addressed; electronic mail: m.g.kong@lboro.ac.uk

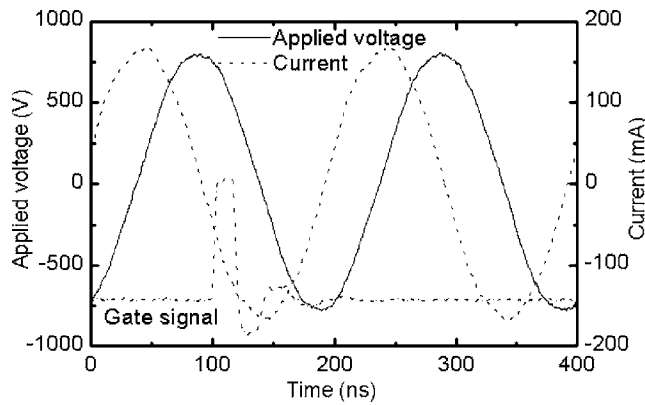


FIG. 1. Trace of the applied voltage and the discharge current of a rf DBD in an atmospheric helium flow, together with the iCCD trigger signal.

barriers, Fig. 2 shows the current-voltage characteristics of the rf APGD and the rf DBD. In the case of the rf APGD, breakdown occurs at an applied voltage of $V_{a,rms}=276.2$ V and $I_{rms}=50.2$ mA. As the applied voltage is increased further, the discharge current grows almost linearly until a transition point of $V_{a,rms}=470.3$ V and $I_{rms}=102.5$ mA, where the glow discharge of 20 mm in diameter shrinks into a narrow constricted column of about 1 mm in diameter. The transition from the constriction point to point *b* in Fig. 2 is rapid and abrupt, similar to those reported elsewhere.^{3,8} It is important to emphasize, however, that the rf APGD after the constriction point may not necessarily be in the γ mode since the γ mode can be achieved without plasma constriction.^{5,9} In fact, the γ mode of unconstricted rf APGD is characterized with a negative differential conductivity of the V_g - J curve, with V_g being the gas voltage and J being the discharge current density.^{5,9} In practice, rf APGD's are susceptible to plasma constriction and the constricted plasma column tends to be too unstable for its current density to be estimated reliably. While more studies are needed to establish whether the constricted plasma is in the γ mode, it is unreliable to use plasma constriction as the indicator of the γ mode.

By adding one ceramic sheet to the plasma-facing side of each electrode and adjusting the gas gap to 2.4 mm, the gas breakdown now occurs at $V_{a,rms}=319.0$ V and $I_{rms}=50.2$ mA. After breakdown, the discharge current in-

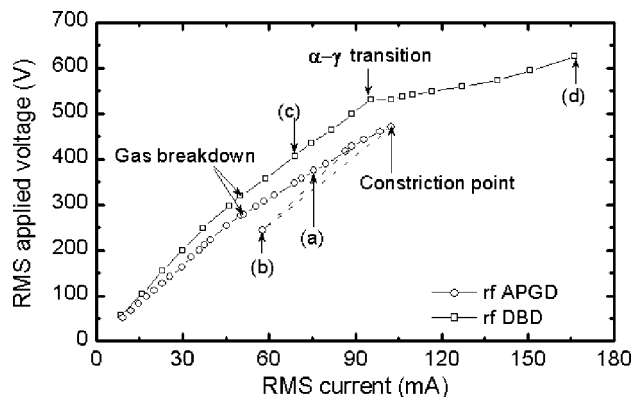


FIG. 2. Current-voltage characteristics of the atmospheric rf DBD and the rf APGD, marked with the gas breakdown point, the plasma constriction point, and the α - γ mode transition point. Points (a), (b), (c), and (d) indicate conditions where plasma images in Figs. 3 and 4 were taken. The dashed line indicates conditions of plasma constriction.

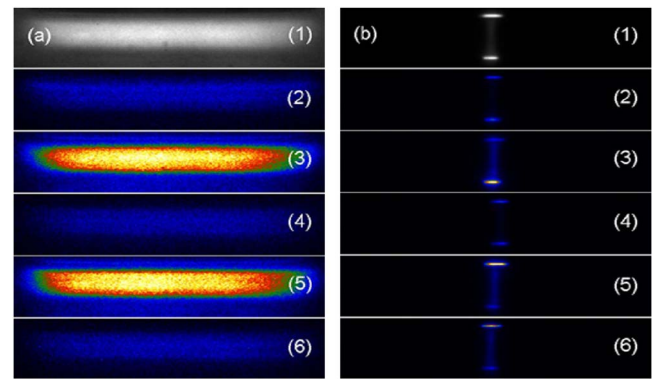


FIG. 3. (Color online) Plasma images of the rf APGD at (a) $I_{rms}=75.7$ mA and point *a* in Fig. 2 and (b) $I_{rms}=57.8$ mA and point *b* in Fig. 2. The images in (1) were taken with 1 ms exposure time. Images in (2), (3), (4), (5), and (6) were taken with 10 ns exposure time at $t=0$, $T/4$, $2T/4$, $3T/4$, and T , respectively, with T being the rf cycle period.

creases with increasing applied voltage. For a given discharge current, the applied voltage of the rf DBD is always larger than that of the rf APGD and their difference increases with increasing discharge current. This is because the dielectric barriers divide into the applied voltage and the total voltage across the barriers, $V_{m,rms}$, increases with the current due to $V_{m,rms}=I_{rms}/\omega C_m$, with C_m being the total barrier capacitance. As the applied voltage increases further, a step change in the differential conductivity in the $V_{a,rms}$ - I_{rms} curve is apparent at 530.4 V and 95.5 mA. As will be shown later, the rf DBD retains its volume above $I_{rms}=95.5$ mA. This suggests that plasma constriction is avoided in the rf DBD and the cross-sectional area of the discharge remains the same over the entire current range. Hence, the differential conductivity criterion⁵ can be invoked. It has been demonstrated that a step change in the differential conductivity of the $V_{a,rms}$ - I_{rms} curve such as that in Fig. 2 is caused by the α - γ mode transition with the differential conductivity of the V_g - J curve changing from positive to negative.¹² Therefore, the rf DBD above $I_{rms}=95.5$ mA in Fig. 2 is in the γ mode and the point at $I_{rms}=95.5$ mA is the α - γ mode transition point. It is clear that the use of dielectric barriers mitigates plasma constriction in rf atmospheric glow discharges and expands them into regimes of large discharge currents. The experimental evidence of plasma constriction control and the α - γ mode transition in Fig. 2 agrees very well qualitatively with our numerical prediction.¹²

To provide further support to the above discussion, images of the rf APGD and the rf DBD were taken by the iCCD camera. Figure 3(a) shows a millisecond image of the rf APGD and its five nanosecond images at $I_{rms}=75.7$ mA corresponding to point *a* in Fig. 2. Images in (3) and (5) of Fig. 3(a) were taken at the instants of $t=T/4$ and $3T/4$ when the discharge current reached its positive and negative maxima. It is clear that the rf APGD is horizontally homogeneous. Its optical emission covers the majority of the gas gap with the peak optical signal located in the gap center. This suggests a volumetric discharge with a bell-like profile of optical emission centered at the middle of the gas gap. These features are characteristic of the α mode^{5,9,15} and provide experimental confirmation of the α mode operation of the rf APGD in the 50.2–102.5 mA range. At point *b* in Fig. 2 and 57.8 mA, Fig. 3(b) shows that the rf APGD is now a constricted plasma column of about 1 mm in diameter. The

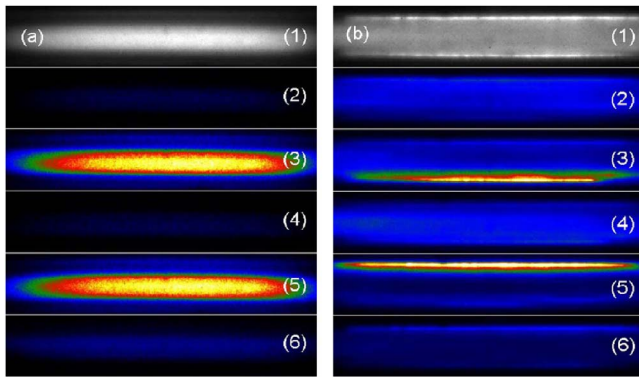


FIG. 4. (Color online) Plasma images of the rf DBD at (a) $I_{\text{rms}}=69.0$ mA and point *c* in Fig. 2 and (b) $I_{\text{rms}}=166.2$ mA and point *d* in Fig. 2. The images in (1) were taken with 1 ms exposure time. Images in (2) (3), (4), (5), and (6) were taken with 10 ns exposure time at $t=0$, $T/4$, $2T/4$, and $3T/4$, respectively.

constricted plasma is unstable, moving around, as shown in the nanosecond images of (2)–(6) in Fig. 3(b). This confirms that the rf APGD is susceptible to plasma constriction and its constriction is evolved from the α mode directly.

After the dielectric barriers are introduced, plasma constriction is avoided. Figure 4(a) shows a millisecond image of the rf DBD and its five nanosecond images at $I_{\text{rms}}=69.0$ mA corresponding to point *c* in Fig. 2. Images in (3) and (5) were taken at the instants of $t=T/4$ and $3T/4$ when the discharge current reached its positive and negative maxima. Similar to Fig. 3(a), the discharge is horizontally homogeneous, covering the gas gap with a bell-like profile. This is characteristic of the α mode.^{5,9,15} As the current is increased to $I_{\text{rms}}=166.2$ mA corresponding to point *d* in Fig. 2, images in Fig. 4(b) suggest that the rf DBD retains the same volume as that in Fig. 4(a) and plasma constriction is avoided. The discharge is again horizontally homogeneous but now exhibits localized gas ionization. The image in (3) in Fig. 4(b) shows a thin bright layer very close to the instantaneous cathode (the bottom electrode), whereas the image in (5) shows a similar bright layer near the instantaneous anode (the top electrode). These are the negative glow and indicate localized gas ionization near the sheath bulk, thus offering a direct evidence of the γ mode. Figure 4 supports further that dielectric barriers can mitigate plasma constriction and enable the γ mode of rf atmospheric glow discharges over a large current range.

A typical optical emission spectrum of the rf DBD is shown in Fig. 5(a) from 200 to 800 nm at $I_{\text{rms}}=104.4$ mA. Among the dominant lines are the OH lines at 309 and 617 nm, N_2 at 337 nm, N_2^+ at 357, 391, and 427 nm, O at 777 nm, and He at 706 nm. Although only helium gas was used, the nitrogen and oxygen emission lines were caused by the residual air in the Perspex box and by impurity gases in the helium gas. In rf APGD (Ref. 9) and medium-pressure rf glow discharges,¹¹ the voltage dependence of the electron density has been used to identify the α - γ mode transition. Since the electron density is yet to be measured reliably for rf APGD, we use the optical intensity of the helium line at

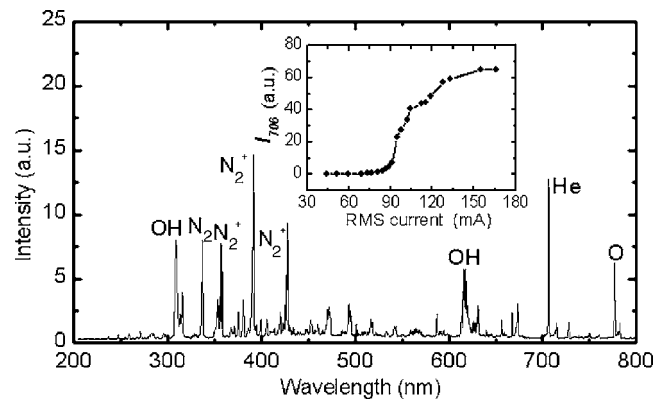


FIG. 5. Optical emission spectrum of the rf DBD at $I_{\text{rms}}=104.4$ mA, with the insert being the current dependence of the 706 nm line intensity.

706 nm as an indirect measure since it is linked to either energetic electrons or He_2^+ and low energy electrons.¹⁶ As shown in Fig. 5(b), the 706 nm line intensity changes little until $I_{\text{rms}}=91.2$ mA after which it grows rapidly with the discharge current. The corner point of $I_{\text{rms}}=91.2$ mA is not dissimilar to the α - γ transition point of $I_{\text{rms}}=95.5$ mA in Fig. 2, supporting further that the γ mode has indeed been achieved in the rf DBD without plasma constriction.

In conclusion, we have shown that plasma constriction common to rf APGD can be mitigated with dielectrically insulated electrodes. The resulting atmospheric rf DBD can operate in the γ mode of very large discharge currents while retaining their volume. Atmospheric rf DBD's are capable of greater plasma stability than rf APGD's and so offer a brighter prospect to a wide range of applications.

This work was funded partly by Engineering and Physical Science Research Council, U.K. and partly by Department of Health, UK.

¹S. E. Babayan, G. Ding, G. R. Nowling, X. Yang, and R. F. Hicks, *Plasma Chem. Plasma Process.* **22**, 255 (2002).

²L. Baars-Hibbe, P. Sichler, C. Schrader, C. Gessner, K. H. Gericke, and S. Buttgenbach, *Surf. Coat. Technol.* **174**, 519 (2003).

³J. J. Shi, X. T. Deng, R. Hall, J. D. Punnett, and M. G. Kong, *J. Appl. Phys.* **94**, 6303 (2003).

⁴A. P. Yalin, Z. Q. Yu, O. Stan, K. Hoshimiya, A. Rahman, V. K. Surla, and G. J. Collins, *Appl. Phys. Lett.* **83**, 2766 (2003).

⁵J. J. Shi and M. G. Kong, *IEEE Trans. Plasma Sci.* **33**, 624 (2005).

⁶R. Foest, E. Kindel, A. Ohl, M. Stieber, and K. D. Weltmann, *Plasma Phys. Controlled Fusion* **47B**, 525 (2005).

⁷W. C. Zhu, B. R. Wang, Z. X. Yao, and Y. K. Pu, *J. Phys. D* **38**, 1396 (2005).

⁸S. Y. Moon, J. W. Han, and W. Choe, *Phys. Plasmas* **13**, 013504 (2006).

⁹J. J. Shi and M. G. Kong, *J. Appl. Phys.* **97**, 023306 (2005).

¹⁰J. J. Shi and M. G. Kong, *Appl. Phys. Lett.* **87**, 201501 (2005).

¹¹Y. P. Raizer, M. N. Shneider, and N. A. Yatsenko, *Radio-frequency Capacitive Discharges* (CRC, Boca Raton, FL, 1995), p. 264.

¹²J. J. Shi, D. W. Liu, and M. G. Kong, *Appl. Phys. Lett.* **89**, 081502 (2006).

¹³I. Radu, R. Bartnikas, and M. R. Wertheimer, *IEEE Trans. Plasma Sci.* **31**, 411 (2003).

¹⁴M. G. Kong and X. T. Deng, *IEEE Trans. Plasma Sci.* **31**, 7 (2003).

¹⁵J. J. Shi and M. G. Kong, *Phys. Rev. Lett.* **96**, 105009 (2006).

¹⁶N. K. Bibinov, A. A. Fateev, and K. Wiesemann, *J. Phys. D* **34**, 1819 (2001).